An urban trees parameterization for modelling microclimatic variables and thermal comfort conditions at street level with the Town Energy Balance model (TEB-SURFEX v8.0)

Redon Emilie[1], Lemonsu Aude[1], and Masson Valéry[1]

[1]CNRM, Météo-France/CNRS, 42 avenue Gaspard Coriolis, 31057 Toulouse cedex, France

Correspondence: Aude Lemonsu (aude.lemonsu@meteo.fr)

Abstract. The Town Energy Balnce (TEB) urban climate model has recently been improved to more realistically address the radiative effects of trees within the urban canopy. These processes necessarily have an impact on the energy balance that needs to be taken into account. This is why a new method for calculating the turbulent fluxes for sensible and latent heat has been implemented. This method remains consistent with the "bigleaf" approach of the Interaction Soil-Biosphere-Atmosphere (ISBA) model which deals with energy exchanges between vegetation and atmosphere within TEB. Nonetheless, the turbulent fluxes can now be dissociated between ground-based natural covers and tree stratum above (knowing the vertical leaf density profile), which can modify the vertical profile in air temperature and humidity in the urban canopy. In addition, the aeraulic effect of trees is added, parameterized as a drag term and an energy dissipation term in the evolution equations of momentum and of turbulent kinetic energy, respectively. This set of modifications relating to the explicit representation of tree stratum in TEB is evaluated on an experimental case study. The model results are compared to micrometeorological and surface temperature measurements collected in a semi-open courtyard with trees and bordered by buildings. The new parameterizations improve the modelling of surface temperatures of walls and pavements thanks to taking into account radiation absorption by trees, and of air temperature. The wind speed is strongly slowed down by trees that is also much more realistic. The universal thermal climate index diagnosed in TEB from inside-canyon environmental variables is highly dependent and sensitive to these variations in wind speed and radiation. This demonstrates the importance of properly modelling interactions between buildings and trees in urban environments, especially for climate-sensitive design issues.

Copyright statement. TEXT

1 Introduction

The urban climate commonly refers to the modification of local climate by the urban environment. It results from the establishment of radiative, energetic, dynamic, hydrological surface processes that are pecular to urban covers properties (Oke et al., 2017). This urban climate may however present important spatial variabilities within the city. The street-level meteorological variables, i.e. air temperature, humidity, wind, are modified in by the local environment depending the morphology and

arrangement of buildings, the surface properties and more generally the land covers composition (Houet and Pigeon, 2011; Fenner et al., 2014; Ndetto and Matzarakis, 2014; Alexander and Mills, 2014).

The presence of vegetation, and especially urban trees, is one element of modification of local microclimate (Bernatzky, 1982; Oke, 1989; Shashua-Bar and Hoffman, 2000; Potchter et al., 2006; Shashua-Bar et al., 2011). The trees functioning is governed by own physiological processes together with local environmental conditions. When located in a street canyon, the trees come in interaction with the surrounding urban elements. The radiative exchanges are modified as well as energy fluxes and local air flows. The incoming radiation is intercepted by the tree foliage depending on its localization and coverage in the street (Souch, 1993; Armson et al., 2012; Berry et al., 2013). It is for one part reflected upward according to reflective properties of leaves, whereas the other part is partially transmitted through the foliage or absorbed by it. The scattering modulates the properties of reflected and transmitted radiation. The multiple reflections of short- and long-wave radiation between all components of the canyon are also disrupted by the presence of trees that are furthermore an additional source of infrared emissions. A part of energy absorbed by trees is used in the transpiration process associated to photosynthesis (Peters et al., 2011; Qiu et al., 2013). This is a water exchange from aerial parts of plants to the atmosphere through stomata. The transpiration rate is related to the stomata opening level which is regulated according to environmental conditions of sunlight, temperature, humidity and wind, but also to soil water availability (Konarska et al., 2016; Litvak and Pataki, 2016). As a consequence, the energy exchanges that are mostly dominated by heat transfers through conduction and convection in built-up environments can be significantly modified with the vegetation effects (Grimmond et al., 1996; Offerle et al., 2006; Best and Grimmond, 2016). Finally, the trees are physical obstacles to the flow within the street (Heisler, 1990; Giometto et al., 2017; Martini et al., 2017). They lead to a drag effect on the mean flow and modify local turbulent exchanges which can have an impact on ventilation as well as on particles dispersion (Buccolieri et al., 2011; Abhijith et al., 2017).

Some of urban climate models are capable to simulate the presence of certain vegetated elements in the urban environment. They are not represented with the same level of accuracy, nor the same physical processes. The high spatial resolution softwares or models that are based on near-reality numerical mock-ups of the environment integrate trees as fully elements composing the scene simulated as porous media (Bruse and Fleer, 1998; Salim et al., 2015). They are obstacles on the same level as buildings, and can consequently be involved in dynamical processes in CFD modelling. They are resolved explicitly in some radiative transfer models such as SOLENE (Miguet and Groleau, 2007) or DART (Gastellu-Etchegorry et al., 1996). They are here described as turbid objects that intercept, transmit, absorb, and emit radiation, in complex interaction between all surrounding objects of the scene.

Some of urban canopy models coupled or implemented in meso-scale atmospheric models now include a representation of urban vegetation and even of trees. This is done through a simplified approach for which trees effects are parameterized (Lee and Park, 2008; Krayenhoff et al., 2014, 2015; Ryu et al., 2016; Redon et al., 2017). Despite a simplified description of the urban environment, the main physical processes can be taken into account, i.e. radiation interactions between a mean tree foliage layer within the canyon and surrounding urban facets, the modification of wind profile within the canyon by drag effect of this foliage layer, or the transpiration of trees. These models offer the interest to be able to apply over the whole city and to operate in complete three-dimensional atmospheric simulations where two-ways interactions between complex surfaces and

atmosphere are resolved. They have then the capability to simulate a certain level of microclimate variability between neighbourhoods (de Munck et al., 2018) especially according to the presence of vegetation and trees, and the potential influences or interferences between local microclimates by horizontal advection.

2 Representation of natural covers in TEB

2.1 Previous developments and general approach

The Town Energy Balance (TEB) urban canopy model is one of the first model from this generation to have included urban vegetation in local-scale interaction with the built-up elements. It has been progressively made more complex by integrating new types of nature elements and new associated processes. The first step was the inclusion of ground-based vegetation within the canyon by implementing the Interaction Soil-Biosphere-Atmosphere (ISBA, Noilhan and Planton, 1989) model within TEB (Lemonsu et al., 2012). ISBA is a surface-vegetation-atmosphere transfer (SVAT) model. This coupling makes it possible to simulate the physiological behaviour of plants subject to radiative effects of urban geometry and to microclimate conditions of the urban environment. Reversely, the microclimate within the canyon can be impacted by the modification of surface energy exchanges due to the presence of vegetation at the ground, especially by its evapotranspiration. A module of extensive green roofs was also developed (de Munck et al., 2013) still using the ISBA model to simulate the hydrological and energetic functioning of the green roofs, as well as the energy exchanges with atmosphere and the thermal coupling with the buildings on which they are installed.

2.2 Radiative effects of urban trees

Finally the most recent developments regard trees. Redon et al. (2017) proposed a new parameterization for modelling the radiative effects of trees by including a tree-foliage stratum within the urban canyon which can partially cover ground-based surfaces. The positioning and geometry of individual trees are not described explicitly but rather approached as (1) an horizontal coverage fraction within the canyon, (2) a vertical thickness by defining a mean height of trees and a mean height of trunks, and (3) a mean leaf density profile (see description in Figure 1). The trees foliage can intercept a part of incoming radiation depending on canyon geometry, that is either reflected upward, or transmitted through the foliage, or absorbed by the foliage. In addition, the foliage layer takes part of radiation inter-reflections within the canyon between the different components (trees, walls, road, ground-based natural covers) and contributes to infrared emissions. Separated calculations are done for direct and diffuse components of shortwave radiation, and for long-wave radiation. The direct shortwave radiation is assumed directional whereas the diffuse shortwave radiation, the longwave radiation, and any radiation after reflection are assumed to be isotropic. The radiation interactions between all components of the canyon are consequently managed using form factors calculated between all of them.

These developments were evaluated by comparison with solar enlightenment modelling performed by a high-resolution archi-

tectural software, for a large set of simple-geometry urban canyons, with various aspect ratios and various trees arrangements within (Redon et al., 2017). Due to the simplified representation of trees geometry, a general defect is the underestimatation of the incoming solar radiation interception by the tree-foliage stratum. That is explained by the fact that TEB does not represent the sides of tree crowns, that can receive in reality a part of incoming radiation according to their position and inclination of the sun's rays. The simplified approach is also a limitation for describing some vegetation arrangements such as multiple lanes of trees. Nonetheless, the results are quite acceptable and confirm this new version make possible to better simulate the radiative interactions in canyons with trees.

In coherence with this explicit separation of vegetation strata, there was then a need to adapt the calculation of the turbulent fluxes related to low and high vegetation as well as to include the drag effect of trees on wind profile in the canyon. These new developments and their evaluation by comparison to microclimatic measurements are presented and discussed here. There are complemented by an updated calculation of the universal thermal comfort index (UTCI) by including the effect of trees.

3 Surface energy balance of the canyon components in TEB

3.1 Descripion of natural covers with the "bigleaf approach"

The TEB model resolves the radiative budget for each component of the urban canyon. In the case of a treeless canyon, it accounts for obstruction effects due to buildings in calculation of incoming short- and long-wave radiation interception by roads, walls, and natural ground-based surfaces, as described in details in Masson (2000) and Lemonsu et al. (2012). The new version of Redon et al. (2017) now includes the additional interactions with the tree-foliage stratum. From the resolution of radiation budget, the energy quantity absorbed in short- (S^*) and long-wave (L^*) radiation by each component or net radiation (Q^*) is determined:

$$Q^* = S^* + L^* \tag{1}$$

This net energy source is redistributed as turbulent sensible (Q_H) and latent (Q_E) heat fluxes between each considered component and local atmosphere, and as a storage heat flux by conduction (Q_G) through the component itself (i.e. through the artificial-materials layers that compose the roof, the road or the walls, or in the ground for the natural covers).

For the built-up facets of urban canyon (road, wall, roof), the surface energy balance (SEB) calculations remain unchanged in the TEB model, but with Q^* potentially modified in case of canyons with trees. Since the works of Lemonsu et al. (2012), the turbulent processes for natural parts of the urban canyon (natural soils and ground-based vegetation) are resolved in TEB through the integration of the ISBA model that is here constrained by radiative and microclimatic conditions related to the urban environment. The ISBA model is based on that is called "the bigleaf approach" in which the natural covers are managed as a unique composite compartment. This compartment consists of fractions of bare soil, low vegetation, and high vegetation (and possibly snow). It is characterized by mean properties calculated from thermo-radiative (albedo, emissivity, heat capacity),

aerodynamic (roughness length), and physiological (stomatal resistance for plants) parameters that are prescribed independently for the different types that compose it. A single temperature (T_{nat}) is associated to the compartment, and a single SEB is resolved:

$$Q^*_{nat} = Q_{H_{nat}} + Q_{E_{nat}} + Q_{G_{nat}} \tag{2}$$

5 This net radiation depends on the radiation budget which is expressed as following:

$$Q^*_{nat} = S^*_{nat} + L^*_{nat} = (1 - \alpha_{nat})S^\downarrow_{nat} + \epsilon_{nat}(L^\downarrow_{nat} - \sigma T^4_{nat}) \tag{3}$$

The incoming short- and long-wave radiation intercepted by natural covers compartment ($S^\downarrow_{nat}$ and $L^\downarrow_{nat}$) are calculated for a reference level at the ground within the urban canyon. The composite albedo (α_{nat}) is calculated as an average of bare soil and vegetation albedo (which are themselves average albedos of snow-covered and snow-free surfaces). Same is done for the
10 emissivity (ϵ_{nat}).

3.2 Modification of surface energy balance due to implementation of trees

The implementation of a tree canopy in TEB like a supplementary foliage stratum makes it possible to separate the incoming radiation received by natural covers as a part received by ground-based natural surfaces ($S^\downarrow_g$ and $L^\downarrow_g$) and a part received by trees ($S^\downarrow_t$ and $L^\downarrow_t$), and also to compute the net radiation for both of them (S^*_t and L^*_t). For purpose of simplicity, the
15 bigleaf concept used in ISBA for the SEB calculation and the resolution of the surface-layer temperature evolution equation is here remained. This requires to calculate aggregated radiation fluxes intercepted by the compartment of natural covers which must be provided to ISBA. Considering that the foliage stratum partially overlaps the ground-based surfaces, these fluxes are aggregated according to the cumulative fraction of natural covers, and accounting for the distribution between covers at the ground and trees:

$$20 \quad S^\downarrow_{nat} \quad = \quad \frac{\delta_g S^\downarrow_g + \delta_t S^\downarrow_t}{\delta_g + \delta_t} \tag{4}$$

$$L^\downarrow_{nat} \quad = \quad \frac{\delta_g L^\downarrow_g + \delta_t L^\downarrow_t}{\delta_g + \delta_t} \tag{5}$$

Here, δ_g is the ground-based surface fraction of the canyon covered by gardens (i.e. bare soil and low vegetation) and δ_t is the overlapping fraction of tree stratum. Note that these fractions are not dependant one from the other, so that their sum can be
25 greater than 1 (Figure 1). Both $Q_{H_{nat}}$ and $Q_{E_{nat}}$ fluxes calculated by ISBA for the composite compartment are then simply redistributed in two contributions from ground-based natural covers (Q_{H_g} and Q_{E_g}) and from trees (Q_{H_t} and Q_{E_t}) to insure the energy conservation:

$$Q_{H_g} \quad = \quad Q_{H_t} \quad = \quad Q_{H_{nat}} \tag{6}$$

$$30 \quad Q_{E_g} \quad = \quad Q_{E_t} \quad = \quad Q_{E_{nat}} \tag{7}$$

4 Inclusion of trees in the surface boundary layer parameterization of TEB

4.1 Principle of the surface boundary layer parameterization

The TEB-SBL (SBL referred to as surface boundary layer) parameterization has been implemented in TEB in order to improve the meteorological variable prediction within the urban canyon (Hamdi and Masson, 2008; Masson and Seity, 2009; Lemonsu et al., 2012). TEB-SBL resolves the surface boundary layer for an air volume in the canyon from a system of evolution equations for air temperature (T), specific humidity (q), wind speed (U), and turbulent kinetic energy (E). For taking into account the effects of canyon on the local atmospheric characteristics evolution, an additional forcing term is included in each of these equations, according to the approach proposed by Yamada (1982) for the drag forces related to the vegetation canopies. The equations have the same general expression, with V the considered variable and F_V the general forcing term including advection, Coriolis force, and pressure gradient:

$$\frac{\partial V}{\partial t} = F_V + \left.\frac{\partial V}{\partial t}\right|_{can} \tag{8}$$

The last term to the right is the forcing term due to the canyon. It translates a drag force for the wind, a heating/cooling effect for air temperature, a humidification/dryness effect for air humidity, and a dissipation/production effect for turbulent kinetic energy. According to Martilli et al. (2002), these additional contributions are associated to horizontal and vertical surfaces of the canyon:

$$\left.\frac{\partial V}{\partial t}\right|_{can} = \left.\frac{\partial V}{\partial t}\right|_{can}^H + \left.\frac{\partial V}{\partial t}\right|_{can}^V \tag{9}$$

For these terms, the equations are resolved according to a vertical discretisation of the air volume from the ground to a reference atmospheric level located above the top of buildings (Figure 1). As described by Lemonsu et al. (2012), the equation system of the TEB-SBL parameterization is expressed as following for each k vertical layer :

$$\left.\frac{\partial U(k)}{\partial t}\right|_{can} = -C_{d_{bld}} U(k)^2 \frac{S_{V_w}(k)}{V_{air}} - u_*^2(k) \left(\frac{S_{H_R}(k)}{V_{air}} + \frac{S_{H_r}(k)}{V_{air}} \right) \tag{10}$$

$$\left.\frac{\partial E(k)}{\partial t}\right|_{can} = C_{d_{bld}} U(k)^3 \frac{S_{V_w}(k)}{V_{air}} \tag{11}$$

$$\left.\frac{\partial T(k)}{\partial t}\right|_{can} = \frac{Q_{H_R}}{\rho C_p} \cdot \frac{S_{H_R}(k)}{V_{air}} + \frac{Q_{H_r}}{\rho C_p} \cdot \frac{S_{H_r}(k)}{V_{air}} + \frac{Q_{H_{nat}}}{\rho C_p} \cdot \frac{S_{H_{nat}}(k)}{V_{air}} + \frac{Q_{H_w}}{\rho C_p} \cdot \frac{S_{V_w}(k)}{V_{air}} \tag{12}$$

$$\left.\frac{\partial q(k)}{\partial t}\right|_{can} = \frac{Q_{E_R}}{\rho \mathcal{L}_v} \cdot \frac{S_{H_R}(k)}{V_{air}} + \frac{Q_{E_r}}{\rho \mathcal{L}_v} \cdot \frac{S_{H_r}(k)}{V_{air}} + \frac{Q_{E_{nat}}}{\rho \mathcal{L}_v} \cdot \frac{S_{H_{nat}}(k)}{V_{air}} \tag{13}$$

where $C_{d_{bld}}$ is the drag coefficient for buildings, u_* the friction velocity at level k, V_{air} the air volume of the SBL-scheme layer where exchanges take place, ρ is the air density, and $\mathcal{L}_v$ is the latent heat for vaporization. The sensible heat fluxes of vertical surfaces (Q_{H_w} for walls) contribute to air temperature evolution at layer k relatively to the fraction of the total wall surface in contact with the considered air layer ($S_{V_w}(k)$). The sensible heat fluxes of horizontal surfaces combine Q_{H_R}, Q_{H_r},

and $Q_{H_{nat}}$ for roofs, road, and natural covers, respectively. The roofs only contribute to air temperature for vertical level above building top (with surface S_{H_R}). The contributions of road and of natural covers are here included at the ground-level so that they affect only the first layer of TEB-SBL (with respective surfaces $S_{H_r}(k)$ and $S_{H_{nat}}(k)$). The same types of contributions are parameterized for humidity but in the form of latent heat fluxes.

The vertical transport of heat, humidity and momentum within and above the canyon is calculated by applying the turbulence scheme of Cuxart et al. (2000). This scheme is based on an equation for the turbulent kinetic energy, and is closed with a mixing length. This is parameterized in TEB on the basis of the work of Santiago and Martilli (2010) according to the height of buildings, the mean frontal area density, and the displacement height, i.e. parameters depending on the geometry of the canyon (see Eq. 10-12 in Lemonsu et al., 2012).

4.2   Distribution of heat and humidity fluxes from natural covers

The implementation of trees in TEB requires to modify the ensemble of equations in order to take into account the vertical redistribution of turbulent fluxes and the drag effect of the foliage layer. The turbulent fluxes of trees (Q_{H_t} and Q_{E_t}) coming from the desaggregation of ISBA fluxes calculated with the bigleaf concept (see Eq 6 and 7) are assumed to be produced not at ground-level but at height of the foliage layer within the canyon. These fluxes have therefore to be vertically distributed in the TEB-SBL equations that is here parameterized according to a function of the foliage density contained in each k layer:

$$Q_{H_t}(k) = \int_k LAD(z)dz\, Q_{H_t} = \left(\frac{d_t(k)}{h_t - h_{tk}}\right) LAI\, Q_{H_t} \tag{14}$$

$$Q_{E_t}(k) = \int_k LAD(z)dz\, Q_{E_t} = \left(\frac{d_t(k)}{h_t - h_{tk}}\right) LAI\, Q_{E_t} \tag{15}$$

with $d_t(k)$ is the foliage-layer thickness in the k layer. The leaf area index (LAI in m^2 m^{-2}) is prescribed as input data. The leaf area density (LAD in m^2 m^{-3}) is the vertical profile of LAI which depends on the total thickness of the foliage layer and the form of tree crowns. For now, tree crowns are described rectangular in shape so that LAD is constant over the thickness of tree-foliage layer i.e. between h_{tk} and h_t that are the height of trunks and of trees, respectively.

These turbulent fluxes are now included in the evolution equations of temperature (Eq 12) and humidity (Eq 13) profiles of TEB-SBL, in addition to ground-based contributions coming from natural soils and low-level vegetation:

$$\left.\frac{\partial T(k)}{\partial t}\right|_{can} = \frac{Q_{H_R}}{\rho C_p}\frac{S_{H_R}(k)}{V_{air}} + \frac{Q_{H_r}}{\rho C_p}\frac{S_{H_r}(k)}{V_{air}} + \frac{Q_{H_g}}{\rho C_p}\frac{S_{H_g}(k)}{V_{air}} + \frac{Q_{H_w}}{\rho C_p}\frac{S_{V_w}(k)}{V_{air}} + \frac{Q_{H_t}(k)}{\rho C_p}\frac{V_{grid}}{V_{air}}\delta_t \tag{16}$$

$$\left.\frac{\partial q(k)}{\partial t}\right|_{can} = \frac{Q_{E_R}}{\rho \mathcal{L}_v}\frac{S_{H_R}(k)}{V_{air}} + \frac{Q_{E_r}}{\rho \mathcal{L}_v}\frac{S_{H_r}(k)}{V_{air}} + \frac{Q_{E_g}}{\rho \mathcal{L}_v}\frac{S_{H_g}(k)}{V_{air}} + \frac{Q_{E_t}(k)}{\rho \mathcal{L}_v}\frac{V_{grid}}{V_{air}}\delta_t \tag{17}$$

with δ_t the overlapping fraction of trees in the canyon, and V_{grid} the total air volume.

4.3 Aerodynamic effect of trees

The presence of trees also modifies the air flow within the canyon. For account to this, a supplementary drag term is now included in the evolution equations of momentum (Eq 10) and turbulent kinetic energy (Eq 11):

$$\left.\frac{\partial U(k)}{\partial t}\right|_{can} = -C_{d_{bld}} U(k)^2 \frac{S_{V_w}(k)}{V_{air}} - u_*^2(k)\left(\frac{S_{H_R}(k)}{V_{air}} + \frac{S_{H_r}(k)}{V_{air}}\right) - C_{d_t} U(k)^2 LAD(k)\delta_t \tag{18}$$

$$\left.\frac{\partial E}{\partial t}\right|_{can} = C_{d_{bld}} U(k)^3 \frac{S_{V_w}(k)}{V_{air}} + C_{d_t} U(k)^3 LAD(k)\delta_t \tag{19}$$

Numerous studies found in literature (Cassiani et al., 2008; Dupont and Brunet, 2008; Aumond et al., 2013; Krayenhoff et al., 2015) propose an optimized value of the drag coefficient of trees (C_{d_t}). Until the works of Katul et al. (1998), this coefficient is usually defined as a constant $C_{d_t} = 0.20$.

5 Parameterization of universal thermal climate index

5.1 General principle

The UTCI calculation according to the polynomial regression equation proposed by Bröde et al. (2012) (not detailed here) requires four meteorological parameters: air temperature at 2 m above the ground, the water vapor pressure at the same level, the wind speed at 10 m above the ground, and the mean radiant temperature (T_{mrt}). This equation has been implemented in TEB (Kwok et al., 2019, supplementary materials) for calculating three UTCIs that are associated with a person (1) in the street exposed to the sun, (2) in the street in the shadow, and (3) in the building.

For outdoor conditions in case of a person in the sun, T_{mrt} is calculated by accounting for the ensemble of radiation sources received by the person, i.e. the direct and diffuse incoming short-wave radiation ($S^\downarrow$ and $S^\Downarrow$), the short-wave radiation after reflection on the walls, the road, and the ground-based natural covers in the canyon (S_w^r, S_r^r, S_g^r), the incoming atmospheric long-wave radiation ($L^\downarrow$), and the infrared emissions from surrounding canyon surfaces ($L_w^\uparrow$, $L_r^\uparrow$, $L_g^\uparrow$ for walls, roads, and ground-based natural covers).

The direct short-wave radiation assumed to be unidirectional is weighted by a factor of projected area relative to the person (f_p) which depends on sun elevation (γ in °) according to the formulation of Fanger (1970):

$$f_p = 0.308 \, cos\left\{\gamma\left(1 - \frac{\gamma^2}{48402}\right)\right\} \tag{20}$$

The other fluxes that are considered to be isotropic in TEB radiative calculations are weighted by the form factors calculated for the person (b index is used for $body$) in relation to the surrounding elements that contribute to radiation, i.e. Ψ_{bs}, Ψ_{br}, Ψ_{bw} for the sky, the road, and the walls, respectively (ground-based natural covers have the same form factor than road). Finally,

the mean radiant temperature for the person in the sun is expressed according to the expression:

$$T_{mrt} = \sqrt[4]{\frac{a_b}{\sigma \epsilon_b} \left(\frac{f_p}{sin(\gamma)} S^{\downarrow} + \Psi_{bs} S^{\Downarrow} + \Psi_{bw} S_w^r + \delta_r \psi_{br} S_r^r + \delta_g \psi_{br} S_g^r + \Psi_{bs} L^{\downarrow} + \psi_{bw} L_w^{\uparrow} + \delta_r \psi_{br} L_r^{\uparrow} + \delta_g \psi_{br} L_g^{\uparrow} \right)} \qquad (21)$$

In this expression, the human body is characterized by a prescribed solar absorption coefficient ($a_b = 0.70$) and a prescribed emissivity ($\epsilon_b = 0.97$). In case the person is in the shadow, the term relative to direct short-wave radiation contribution is not taken into account, so that the expression becomes:

$$T_{mrt} = \sqrt[4]{\frac{a_b}{\sigma \epsilon_b} \left(\Psi_{bs} S^{\Downarrow} + \Psi_{bw} S_w^r + \delta_r \psi_{br} S_r^r + \delta_g \psi_{br} S_g^r + \Psi_{bs} L^{\downarrow} + \psi_{bw} L_w^{\uparrow} + \delta_r \psi_{br} L_r^{\uparrow} + \delta_g \psi_{br} L_g^{\uparrow} \right)} \qquad (22)$$

5.2 Inclusion of tree effects

The new parameterization for trees in the TEB model requires to adapt the radiative contributions in the UTCI calculations for outdoor conditions. First, the initial contributions in diffuse short-wave radiation and infrared radiation (detailed in Eq 21) are corrected for the sky and the walls from the radiation attenuation effect through the tree foliage. These attenuation coefficients are those already presented in Redon et al. (2017) that are dependent on the leaf area density profile; they are referred to as τ_{sr} for attenuation between sky and road and τ_{wr} for attenuation between wall and road (see Eq B1-B4 in Redon et al., 2017).

In addition, the tree foliage contributes himself to the total infrared flux received by the person, due to is own infrared emission (function of its temperature and its emissivity) and to the reemission of infrared radiation that it receives from ground and walls. One can note that Redon et al. (2017) made the hypothesis that the short-wave radiation received by tree foliage is only reemitted upward. As a result, no contribution in diffuse short-wave radiation from trees is involved in the mean radiant temperature calculation. The final expression for a person in the sun is as following:

$$T_{mrt} = \sqrt[4]{\frac{a_b}{\sigma \epsilon_b} \left(\frac{f_p}{sin(\gamma)} S^{\downarrow} + \tau_{sr} \Psi_{bs} S^{\Downarrow} + \tau_{wr} \Psi_{bw} S_w^r + \delta_r \psi_{br} S_r^r + \delta_g \psi_{br} S_g^r + \tau_{sr} \Psi_{bs} L^{\downarrow} + \tau_{wr} \psi_{bw} L_w^{\uparrow} + \delta_r \psi_{br} L_r^{\uparrow} + \delta_g \psi_{br} L_g^{\uparrow} + \psi_{bt} L_t^{\uparrow} \right)} \; (23)$$

The infrared emission contribution due to the the tree foliage is expressed as:

$$L_t^{\uparrow} = (1 - \tau_{sr}) \left\{ \sigma \epsilon_t T_t^4 + (1 - \epsilon_t) \Psi_{tr} (\delta_r L_r^{\uparrow} + \delta_g L_g^{\uparrow}) + (1 - \epsilon_t)(1 - \Psi_{tr}) L_w^{\uparrow} \right\} \qquad (24)$$

with ϵ_t and T_t the emissivity and temperature of the tree foliage, respectively, and Ψ_{tr} the form factor for tree regarding emission coming from the road and ground-based natural covers.

6 Evaluation of vegetated-canyon microclimate modelling under semi-arid conditions

An evaluation exercise of the TEB performances in simulating microclimatic conditions of an urban canyon with trees is performed for a real study case, i.e. the experimental campaign presented by Shashua-Bar et al. (2009). The TEB model here applied includes the ensemble of developments relative to urban trees: (1) the radiative processes detailed by Redon et al. (2017) and already evaluated by comparison with a reference model, (2) the energy exchanges between trees and air volume within

the canyon, and (3) the aerodynamic effect of trees on local airflow. This version is referred to as TEB-Tree and is compared to the reference version of the model TEB-Ref (Lemonsu et al., 2012) which already integrated natural covers within the canyon but like a ground-based located compartment.

6.1 Study area and experimental data

5 The experimental data have been collected on campus of Sde-Boqer in the semi-desert region of Negev of southern Israel (30.85°N, 34.78°E, 475 m of altitude) during summer 2007 (Shashua-Bar et al., 2009). Two semi-adjacent courtyards with comparable characteristics in terms of geometry and materials have been set-up according to six landscape arrangments incorporating various combinations of bare soil, lawn, and trees. The cases here studied are the courtyard arranged with trees and bare ground, and the one arranged with trees and grass, respectively referred to as TREE-BARE and TREE-GRASS according

10 to Shashua-Bar et al. (2011). The trees are a *Prosopis juliflora* and a *Tipuana tipu*, that are common species for the region and are known to be water-consumption saving (Shashua-Bar et al., 2009). A drip irrigation was installed for each tree around the trunk. The lawn is *Durban grass* watered separately by sprinklers once in the morning.

The courtyards were equipped with sensors recording (1) air temperature, relative humidity, vapour pressure and wind speed
15 at 1.5 m above the ground, (2) radiation fluxes (incoming and outgoing radiation, and net radiation) at the roof top, (3) surface temperatures of eastern, western, and southfacing walls, and tree foliage, as well as soil and pavement for TREE-BARE and grass for TREE-GRASS, and (4) transpiration from the trees using the sap flow method for both cases and evaporation from the grass with mini-lysimeters for TREE-GRASS. A meteorological station located 400 m northwest of the site in an open desert area recorded for the same period air temperature and humidity at 1.5 m above the ground, wind speed and direction at
20 10 m, as well as soil temperature.

6.2 Numerical configuration and experiments

The simulations are performed by running TEB on a single grid point to which are attributed the descriptive parameters of the experimented courtyards considering their configuration are close to the concept of urban canyon applied in TEB. The TEB model input parameters are prescribed according to the detailed description of the site proposed by Shashua-Bar et al. (2009).
25 The semi-enclosed courtyard are oriented with an angle of 12 ° from the north (clockwise). Their width is 5.5 m and thery are bordered by two rows of three-meters tall buildings with flat roofs. These buildings are made of light concrete, as well as the pavement made of thin layers of light concrete laying on the ground. All impervious covers are light color with high albedo of 0.60 for walls and 0.40 for roofs and pavement. All thermal and radiative properties are listed in Table 1 in Lemonsu et al. (2012). For TREE-BARE, the ground inside of the courtyard consists in 70 % of pavement and 30 % of bare soil. The tree
30 crowns present a overlapping rate of 70 % of ground-based surfaces. For TREE-GRASS, the tree coverage rate is unchanged, while 20 % of the ground is covered by pavement ad 80 % by grass.

The TEB input parameters derived from these real data differ depending on the version TEB-Ref or TEB-Tree that is used

(see the description of configurations in Figure 2 and Table 1). In the TEB-Ref standard approach, land cover fractions are calculated according to a single surface area without overlapping (as seen from the sky or by satellite). The sum of cover fractions is equal to 1. The tree cover has priority over the surfaces that are hidden because located below, which is the case here since the tree-foliage layer covers 70 % of the canyon. In the TREE-BARE experiment, all bare ground and part of pavement are therefore hidden by trees, which modifies the real fractions (Table 1). In the TREE-GRASS experiment, trees largely but not totally mask grass since the grass cover fraction is slightly greater than that of trees (Table 1). In comparison, the TEB-Tree version describes more realistically the arrangement of elements by dissociating the tree-foliage stratum from ground-based natural covers. As a consequence, for both experiments, the cover fractions prescribed for TEB are the real ones (Table 1) and their sum is greater than 1. As for morphological parameters, they remain the same in the two experiments i.e. a wall-plan area ratio of 0.71 and an aspect ratio of 0.55.

The meteorological forcing data that must be provided to TEB, i.e. air temperature, humidity, wind speed, incoming short- and long-wave radiation, and atmospheric pressure above the top of the canyon, are coming from in situ measurements collected above the roof and from data recorded by the reference meteorological station. The method is described in details in Lemonsu et al. (2012).

6.3   Results of evaluation

6.3.1   Microclimatic variables

The results obtained for the TREE-GRASS experiment are presented in detail here by comparing the modelled and measured diurnal cycles of the various parameters documented. They are complemented by the scores obtained for the TREE-BARE experiment. The comparison of microclimatic conditions and surface temperatures observed and simulated within the canyon indicates an improvement of simulation results with the new TEB-Tree version in comparison with TEB-Ref (Figure 3). For air temperature, the improvement brought by TEB-Tree is noted for daytime hours: the simulated diurnal cycle is in better agreement with the observed one. In comparison, the TEB-Ref case indicates a too early warming in the morning. The statistical scores for the whole diurnal cycle (compiled in Table 2) are slightly better with a mean absolute error (MAE) and a root-mean square error (RMSE) of 0.67 and 0.83 $^\circ$C, respectively, instead 0.74 and 0.90 $^\circ$C for TEB-Ref. For the TREE-BARE experiment, the improvement brought by TEB-Tree on air temperature modelling is confirmed by the statistical scores but remains quite low (Table 2). The simulation of the specific humidity is very slightly improved in the TREE-GRASS experiment, but both versions of the model give the same results for the TREE-BARE configuration. In the two experiments whatever the model version, an overall underestimation of humidity is noted, whereas an increase during daytime could reasonably be expected in the new version considering the latent heat flux from natural covers is now vertically distributed in TEB-Tree. The reason of this bias is discussed in the analysis of vertical profiles presented in Section **??**. A clear impact of the new parameterization is observed on wind. By considering the drag effect of tree foliage stratum in equations of TEB-SBL, the air

flow is decelerated. The wind speed simulated in TEB-Tree is significantly lower than in TEB-Ref, that is more conform to measurements. MAE et RMSE are reduced from 1.05 and 1.12 m s^{-1}, respectively, to 0.37 and 0.41 m s^{-1} for TREE-GRASS, and from 1.02 and 1.14 m s^{-1}, respectively, to 0.57 and 0.64 m s^{-1} for TREE-BARE. Nonetheless, an overestimation of wind persists during the day.

6.3.2 Surface temperatures

The wall surface temperatures simulated in TREE-GRASS are significantly improved by taking into account the radiative effects of tree foliage (Figure 3). The incoming radiation received by the canyon facets is reduced due to interception and attenuation by trees that are as tall than buildings. As a result, the surface temperature maxima are lower in TEB-Tree than in TEB-Ref by 4-5 °C for eastern and western walls. Inversely at night, the tree foliage limits the cooling by trapping of infrared emission so that the surface temperatures are higher in TEB-Tree than TEB-Ref. Nonethless despite the improvement, TEB-Tree still overestimates the surface temperature especially for the eastern wall in the morning. This suggests the attenuation effect by tree foliage remains underestimated by the model in this case. The deviation from the measurement can also be explained by a difference between the compared quantities. The thermometer samples a specific area of the wall, while the model calculates an average temperature for the entire wall. The same improvement is noted in TREE-BARE, as well as for pavement temperature that was also measured during the experiment (Table 2).

6.3.3 Trees-related variables

TEB-Ref and TEB-Tree both calculate a composite temperature of natural covers (T_{nat}) which is compared here to the measured foliage temperature (Figure 3f). The foliage presents a much lower diurnal temperature amplitude than that of T_{nat} which is expected since T_{nat} includes a contribution of bare soil or grass depending on the experiment. The evolution of foliage temperature is much better captured by the tree temperature (T_t) diagnosed by TEB-Tree under the simple assumption that the foliage temperature is in equilibrium with the ambient temperature. The comparison between air temperature and foliage measurements confirms that this approximation is quite realistic. Finally, the measured evapotranspiration (combining tree transpiration and grass evaporation) is converted in latent heat flux (Q_E) and compared to model outputs (Figure 4). Until noon, Q_E simulated by TEB-Ref is in good agreement with the observations. But Q_E decreases rapidly to zero in the afternoon, while the measured flux remains positive. TEB-Tree simulates a much higher Q_E during the day that persists up to 6 pm. Even if the day cycle is poorly reproduced in both cases, the daily water quantity evaporated is more realistic with TEB-Tree than with TEB-Ref, since bias is less than 1 % instead -42 % for TEB-Ref.

6.4 Modelling of thermal comfort

An interest of this new parameterization for trees in urban canyons is to better predict outdoor thermal comfort conditions. The air temperature is not so different between the two experiments TEB-Ref and TEB-Tree. The modifications in radiation exchanges, energy fluxes, and ventilation induced by the presence of trees may have nonetheless a significant impact on heat

perception by people. This is here quantified through the UTCI diagnosis whose formulation has been adapted in TEB-Tree in order to include the radiation effects due to tree-foliage stratum as detailed in Section 5.2. Although we do not have any UTCI measurements for direct comparison, it is interesting to study how the two versions of TEB compare. In addition, the model results can be put in perspective with the study of Shashua-Bar et al. (2011) who investigated the influence of trees and grass on outdoor thermal comfort from the same experimental data.

6.4.1   Sensitivity of UTCI to the new TEB-Tree parameterization

The model calculates two separate UTCIs i.e. in the sun and in the shadow. For the analysis of the results, they are averaged in a single UTCI according to the proportion of shade and sunlight in the courtyard. Since the model does not explicitly represent the spatial location of the elements in the canyon but simply coverage fractions, these shade/sun fractions are calculated simply as the ratio between the direct solar radiation received by the ground surface and the direct incident solar radiation at the top of the canyon. TEB-Ref and TEB-Tree are compared in Figure 5 (left) for the TREE-GRASS configuration. Taking into account the foliage layer, TEB-Tree creates much more shade in the courtyard than TEB-Ref which only represents the shade of buildings. Therefore, the UTCI simulated by TEB-Tree is lower during the day than that of TEB-Ref. This difference is 1.8 ° C on average for the daytime hours and reaches 3 ° C at maximum at 2 p.m. For the present study case, it can be seen that the orders of magnitude of the differences in UTCI obtained by comparing the two versions TEB-Ref and TEB-Tree are very significant in terms of predicting heat stress. The TEB-Ref version simulates high heat stress conditions in the middle of the day while TEB-Tree simulates UTCIs do not exceeding moderate heat stress conditions. Inversely during the night, the infrared radiation downward emitted by the tree-foliage stratum in TEB-Tree (and potentially received by a person in the street) significantly limits the decrease in nocturnal UTCI. The UTCI remains on average 1.2 ° C higher than in TEB-Ref simulations. This result is important to be emphasized which highlights that street trees may degrade thermal comfort conditions at night by trapping radiation and amplifying downward infrared emissions inside the canyon while reducing ventilation.

6.4.2   Comparison of comfort conditions depending on courtyard layouts

Shashua-Bar et al. (2011, see Figure 2) compared thermal conditions of the different courtyard layouts based on an index of thermal stress (expressed in W). This index was normalized to smooth the influence of variations in weather conditions from one measurement day to the next. To get closer to these works, UTCIs simulated by TEB-Ref and TEB-Tree for the two configurations TREE-BARE and TREE-GRASS, but also for cases EXPOSED-BARE and EXPOSED-GRASS previously studied by Lemonsu et al. (2012) are compared. These two latter configurations are equivalent to TREE-BARE and TREE-GRASS, respectively, in terms of ground properties but without trees. Identical weather conditions are applied for all courtyard layouts, using those of the TREE-GRASS experiment (Figure 5, right).

It can be seen that the case most exposed to heat stress during the day is the EXPOSED-BARE layout. Thanks to the evapotranspiration of lawn, the EXPOSED-GRASS layout allows local cooling and slightly reduces the UTCI. The two configurations with trees are the most effective during the day: TREE-BARE improves comfort conditions mainly by increasing shade, while

TREE-GRASS combines the benefits of shading and near-surface evapotranspiration. For the studied weather situation, only TREE-GRASS makes it possible to insure moderate heat stress conditions within the courtyard. At night, the treeless configurations allow a more significant lowering of UTCI than those with trees. As already mentioned previously, trees contribute to infrared radiation trapping and are themselves an additional source of radiation. On the other hand, their aerodynamic effect significantly reduces wind speed within the courtyard, which also contributes to limit the decrease in UTCI. These results are in agreement with those of Shashua-Bar et al. (2011, see Figure 2). It is difficult to conclude on the realism of the orders of magnitude for the simulated UTCIs, since indices are not the same in the two studies and the method for comparison or normalization is also different. Nonetheless, whether for the day or night period, the same ranking between configurations in terms of impact on thermal comfort conditions is found. These results are not achievable with the TEB-Ref version, which simulates very similar comfort conditions regardless of the courtyard configuration (not shown).

7 Conclusions

The TEB model has evolved considerably in recent years, particularly with the objective of improving the representation of vegetation in urban areas. After the implementation of ground-based low vegetation inside the canyon, and of green roofs on buildings, an explicit representation of the tree-foliage layer was implemented. A detailed parameterization of associated radiative processes was developed and tested by Redon et al. (2017) with very encouraging results. The whole issue in this study was to treat the energy exchanges of vegetation by taking into account the dissociation of vegetation strata, and to include the drag effect of trees on wind speed in the canyon.

The strategy is rather simple by maintaining the bigleaf approach for using the ISBA SVAT model i.e. by calculating a single energy balance for natural covers, treated as a composite compartment. Nevertheless, the incident radiative fluxes provided to ISBA are calculated as a weighted average of those received by the natural ground surfaces and those received by the trees according to the coverage fractions. The energy fluxes calculated by ISBA are then redistributed according to the same principle between ground surfaces and trees, then injected into the SBL parameterization of TEB for the calculation of the air temperature and humidity vertical profiles of the air in the canyon. Besides, a drag term of trees depending on the horizontal coverage fraction and the leaf density profile of trees is included in evolution equations of momentum and TKE. It is in addition to the drag term already configured for buildings.

An evaluation exercise conducted in comparison to field measurements shows that thanks to these new developments, the model better simulates surface temperatures and air temperature in the canyon. The main improvements concern (1) the wall and ground surface temperatures that are much less overestimated than with the initial parameterization due to tree shading; and (2) the wind which is now slowed down by the presence of trees as observed. There is no very significant effect on air temperature and humidity and it is difficult to conclude on the quality of the turbulent fluxes parameterization. In the future, it could be necessary to move towards a Multi-Energy Budget (MEB) approach (Boone et al., 2017) to solve the energy balance

separately from ground surfaces and trees. The bigleaf approach reveals limitations, and raises conceptual questions about the choice of forcing level for energy fluxes calculations or the representativeness of a single temperature attributed to the composite layer of natural covers.

5 Finally, the UTCI diagnosis was reformulated by taking into account the presence of trees. This essentially consisted of adding infrared emissions from trees to the mean radiant temperature calculation. The other modifications presented here and in Redon et al. (2017) have also an influence on the UTCI because they modify radiative exchanges, and micrometeorological variables in the canyon, particularly wind. The results obtained by comparing different courtyard layouts with and without trees are in accordance with those of Shashua-Bar et al. (2011). The presence of trees improves thermal comfort conditions during the day 10 because of shadow effecs but degrades them during the night. Only the TEB-Tree version is able to correctly simulate these effects that was confirmed by an additional evaluations conducted for another study site in France (de Munck et al., 2018). This underlines the relevance of explicitly taking trees into account in urban climate models in order to more realistically model urban design strategies and impacts on comfort.

Code availability. The TEB code is available in open source via the surface modeling platform SURFEX, downloadable at http://www.umr-
15 cnrm.fr/surfex/. This Open-SURFEX will be updated at relatively low frequency (every 3 to 6 months) and developments presented here are not yet included in the last version. If you need more frequent updates, or if you need what is not in Open-SURFEX (DrHOOK, FA/LFI formats, GAUSSIAN grid), we invite you to follow the procedure to open a GIT account and to access real-time modifications of the code (see instructions in the previous link).

Data availability. The model outputs are available upon request from the corresponding author. The experimental data that are used for the
20 evaluation stage were provided by Prof. Evyatar Erell from Ben-Gurion University of the Negev. To access this data, it is necessary to contact directly Prof. E. Erell.

Author contributions. All three co-authors have contributed to the development and improvement of the TEB's code in SURFEX V8.0. Besides, E. Redon and A. Lemonsu performed the evaluation step by performing the simulation and comparing the model results with the experimental data.

25 *Acknowledgements.* We acknowledge prof. Evyatar Erell from Ben-Gurion University of the Negev for giving us access to the experimental data.

References

Abhijith, K., Kumar, P., Gallagher, J., McNabola, A., Baldauf, R., Pilla, F., Broderick, B., Sabatino, S. D., and Pulvirenti, B.: Air pollution abatement performances of green infrastructure in open road and built-up street canyon environments – A review, Atmospheric Environment, 162, 71 – 86, https://doi.org/https://doi.org/10.1016/j.atmosenv.2017.05.014, http://www.sciencedirect.com/science/article/pii/S1352231017303151, 2017.

Alexander, P. J. and Mills, G.: Local Climate Classification and Dublin's Urban Heat Island, Atmosphere, 5, 755–774, https://doi.org/10.3390/atmos5040755, http://www.mdpi.com/2073-4433/5/4/755, 2014.

Armson, D., Stringer, P., and Ennos, A.: The effect of tree shade and grass on surface and globe temperatures in an urban area, Urban Forestry & Urban Greening, 11, 245 – 255, https://doi.org/https://doi.org/10.1016/j.ufug.2012.05.002, http://www.sciencedirect.com/science/article/pii/S1618866712000611, 2012.

Aumond, P., Masson, V., Lac, C., Gauvreau, B., Dupont, S., and Berengier, M.: Including the Drag Effects of Canopies: Real Case Large-Eddy Simulation Studies, Boundary-Layer Meteorology, 146, 65–80, https://doi.org/10.1007/s10546-012-9758-x, https://doi.org/10.1007/s10546-012-9758-x, 2013.

Bernatzky, A.: The contribution of tress and green spaces to a town climate, Energy and Buildings, 5, 1 – 10, https://doi.org/https://doi.org/10.1016/0378-7788(82)90022-6, http://www.sciencedirect.com/science/article/pii/0378778882900226, 1982.

Berry, R., Livesley, S., and Aye, L.: Tree canopy shade impacts on solar irradiance received by building walls and their surface temperature, Building and Environment, 69, 91 – 100, https://doi.org/https://doi.org/10.1016/j.buildenv.2013.07.009, http://www.sciencedirect.com/science/article/pii/S0360132313002060, 2013.

Best, M. J. and Grimmond, C. S. B.: Modeling the Partitioning of Turbulent Fluxes at Urban Sites with Varying Vegetation Cover, Journal of Hydrometeorology, 17, 2537–2553, https://doi.org/10.1175/JHM-D-15-0126.1, 2016.

Boone, A., Samuelsson, P., Gollvik, S., Napoly, A., Jarlan, L., Brun, E., and Decharme, B.: The interactions between soil–biosphere–atmosphere land surface model with a multi-energy balance (ISBA-MEB) option in SURFEXv8 – Part 1: Model description, Geoscientific Model Development, 10, 843–872, https://doi.org/10.5194/gmd-10-843-2017, https://www.geosci-model-dev.net/10/843/2017/, 2017.

Bröde, P., Fiala, D., Błażejczyk, K., Holmér, I., Jendritzky, G., Kampmann, B., Tinz, B., and Havenith, G.: Deriving the operational procedure for the Universal Thermal Climate Index (UTCI), International Journal of Biometeorology, 56, 481–494, https://doi.org/10.1007/s00484-011-0454-1, https://doi.org/10.1007/s00484-011-0454-1, 2012.

Bruse, M. and Fleer, H.: Simulating surface–plant–air interactions inside urban environments with a three dimensional numerical model, Environmental Modelling & Software, 13, 373 – 384, https://doi.org/https://doi.org/10.1016/S1364-8152(98)00042-5, http://www.sciencedirect.com/science/article/pii/S1364815298000425, 1998.

Buccolieri, R., Salim, S., Leo, L., Di Sabatino, S., Chan, A., Ielpo, P., de Gennaro, G., and Gromke, C.: Analysis of local scale tree–atmosphere interaction on pollutant concentration in idealized street canyons and application to a real urban junction, Atmospheric Environment, 45, 1702–1713, https://doi.org/10.1016/J.ATMOSENV.2010.12.058, https://www.sciencedirect.com/science/article/pii/S1352231011000057, 2011.

Cassiani, M., Katul, G. G., and Albertson, J. D.: The Effects of Canopy Leaf Area Index on Airflow Across Forest Edges: Large-eddy Simulation and Analytical Results, Boundary-Layer Meteorology, 126, 433–460, https://doi.org/10.1007/s10546-007-9242-1, https://doi.org/10.1007/s10546-007-9242-1, 2008.

Cuxart, J., Bougeault, P., and Redelsperger, J.-L.: A turbulence scheme allowing for mesoscale and large-eddy simulations, Quart. J. Roy. Meteorol. Soc., 126(562), 1–30, 2000.

de Munck, C., Lemonsu, A., Bouzouidja, R., Masson, V., and Claverie, R.: The GREENROOF module (v7.3) for modelling green roof hydrological and energetic performances within TEB, Geoscientific Model Development, 6, 1941–1960, https://doi.org/10.5194/gmd-6-1941-2013, https://www.geosci-model-dev.net/6/1941/2013/, 2013.

de Munck, C., Bernard, E., Lemonsu, A., Hidalgo, J., Touati, N., and Bouyer, J.: Impact of modelling vegetation at high resolution on urban climate variability, in: 10th International Conference on Urban Climate (ICUC10), New York City, US, 2018.

Dupont, S. and Brunet, Y.: Edge Flow and Canopy Structure: A Large-Eddy Simulation Study, Boundary-Layer Meteorology, 126, 51–71, https://doi.org/10.1007/s10546-007-9216-3, https://doi.org/10.1007/s10546-007-9216-3, 2008.

Fanger, P. O.: Thermal comfort : analysis and applications in environmental engineering, Copenhagen : Danish Technical Press, 1970.

Fenner, D., Meier, F., Scherer, D., and Polze, A.: Spatial and temporal air temperature variability in Berlin, Germany, during the years 2001–2010, Urban Climate, 10, 308 – 331, https://doi.org/https://doi.org/10.1016/j.uclim.2014.02.004, http://www.sciencedirect.com/science/article/pii/S2212095514000145, iCUC8: The 8th International Conference on Urban Climate and the 10th Symposium on the Urban Environment, 2014.

Gastellu-Etchegorry, J., Zagolski, F., and Romier, J.: A simple anisotropic reflectance model for homogeneous multilayer canopies, Remote Sensing of Environment, 57, 22–38, 1996.

Giometto, M., Christen, A., Egli, P., Schmid, M., Tooke, R., Coops, N., and Parlange, M.: Effects of trees on mean wind, turbulence and momentum exchange within and above a real urban environment, Advances in Water Resources, 106, 154 – 168, https://doi.org/https://doi.org/10.1016/j.advwatres.2017.06.018, http://www.sciencedirect.com/science/article/pii/S0309170817306486, tribute to Professor Garrison Sposito: An Exceptional Hydrologist and Geochemist, 2017.

Grimmond, C., Souch, C., and Hubble, M.: Influence of tree cover on summertime surface energy balance fluxes, San Gabriel Valley, Los Angeles, Climate Research, 6, 45–57, 1996.

Hamdi, R. and Masson, V.: Inclusion of a Drag Approach in the Town Energy Balance (TEB) Scheme: Offline 1D Evaluation in a Street Canyon, Journal of Applied Meteorology and Climatology, 47, 2627–2644, https://doi.org/10.1175/2008JAMC1865.1, 2008.

Heisler, G.: Urban form and climate change: Balancing adaptation and mitigation in the U.S. and Australia, ASHRAE Transactions, 96, 1389–1396, 1990.

Houet, T. and Pigeon, G.: Mapping urban climate zones and quantifying climate behaviors - An application on Toulouse urban area (France), Environmental Pollution, 159, 2180–2192, https://doi.org/10.1016/j.envpol.2010.12.027, https://hal.archives-ouvertes.fr/hal-00561959, 2011.

Katul, G., Geron, C., Hsieh, C.-I., Vidakovic, B., and Guenther, A.: Active Turbulence and Scalar Transport near the Forest–Atmosphere Interface, Journal of Applied Meteorology, 37, 1553–1546, 1998.

Konarska, J., Uddling, J., Holmer, B., Lutz, M., Lindberg, F., Pleijel, H., and Thorsson, S.: Transpiration of urban trees and its cooling effect in a high latitude city, International Journal of Biometeorology, 60, 159–172, 2016.

Krayenhoff, E., Christen, A., Martilli, A., and Oke, T.: A Multi-layer Radiation Model for Urban Neighbourhoods with Trees, Boundary-Layer Meteorology, 151, 139–178, https://doi.org/10.1007/s10546-013-9883-1, 2014.

Krayenhoff, E., Santiago, J.-L., Martilli, A., Christen, A., and Oke, T.: Parametrization of Drag and Turbulence for Urban Neighbourhoods with Trees, Boundary-Layer Meteorology, 156, 157–189, https://doi.org/10.1007/s10546-015-0028-6, 2015.

Kwok, Y., Schoetter, Lau, K.-L. L., Hidalgo, J., Ren, C., Pigeon, G., and Masson, V.: How does the local climate zone scheme discern the urban thermal environment? Evaluation for a European city (Toulouse) using numerical simulation data, International Journal of climatology, in revision, 2019.

Lee, S.-H. and Park, S.-U.: A Vegetated Urban Canopy Model for Meteorological and Environmental Modelling, Boundary-Layer Meteorology, 126, 73–102, https://doi.org/10.1007/s10546-007-9221-6, 2008.

Lemonsu, A., Masson, V., Shashua-Bar, L., Erell, E., and Pearlmutter, D.: Inclusion of vegetation in the Town Energy Balance model for modelling urban green areas, Geoscientific Model Development, 5, 1377–1393, https://doi.org/10.5194/gmd-5-1377-2012, 2012.

Litvak, E. and Pataki, D.: Evapotranspiration of urban lawns in a semi-arid environment: An in situ evaluation of microclimatic conditions and watering recommendations, Journal of Arid Environments, 134, 87 – 96, https://doi.org/https://doi.org/10.1016/j.jaridenv.2016.06.016, http://www.sciencedirect.com/science/article/pii/S0140196316301173, 2016.

Martilli, A., Clappier, A., and Rotach, M.: An Urban Surface Exchange Parameterisation for Mesoscale Models, Boundary-Layer Meteorology, 104, 261–304, https://doi.org/10.1023/A:1016099921195, 2002.

Martini, A., Biondi, D., and Batista, A. C.: The microclimate of different landscape arrangements in street trees of Curitiba-pr State, Ciência Florestal, 27, 1257 – 1268, 2017.

Masson, V.: A Physically-Based Scheme For The Urban Energy Budget In Atmospheric Models, Boundary-Layer Meteorology, 94, 357–397, https://doi.org/10.1023/A:1002463829265, 2000.

Masson, V. and Seity, Y.: Including Atmospheric Layers in Vegetation and Urban Offline Surface Schemes, Journal of Applied Meteorology and Climatology, 48, 1377–1397, https://doi.org/10.1175/2009JAMC1866.1, 2009.

Miguet, F. and Groleau, D.: Urban bioclimatic indicators for urban planners with the software tool SOLENE, Portugal SB07 Sustainable Construction, materials and practices: challenges of the industry for the new millennium, Lisbon, Portugal, pp. 348–355, 2007.

Ndetto, E. and Matzarakis, A.: Urban atmospheric environment and human biometeorological studies in Dar es Salaam, Tanzania, Air Quality Atmosphere & Health, https://doi.org/10.1007/s11869-014-0261-z, 2014.

Noilhan, J. and Planton, S.: A Simple Parameterization of Land Surface Processes for Meteorological Models, Monthly Weather Review, 117, 536–549, https://doi.org/10.1175/1520-0493(1989)117<0536:ASPOLS>2.0.CO;2, 1989.

Offerle, B., Grimmond, C., Fortuniak, K., and Pawlak, W.: Intraurban Differences of Surface Energy Fluxes in a Central European City, Journal of Applied Meteorology and Climatology, 45, 125–136, https://doi.org/10.1175/JAM2319.1, 2006.

Oke, T.: The micrometeorology of the urban forest, Philosophical Transactions of the Royal Society of London B: Biological Sciences, 324, 335–349, https://doi.org/10.1098/rstb.1989.0051, 1989.

Oke, T. R., Mills, G., Christen, A., and Voogt, J. A.: Urban Climates, Cambridge University Press, https://doi.org/10.1017/9781139016476, 2017.

Peters, E., Hiller, R., and McFadden, J.: Seasonal contributions of vegetation types to suburban evapotranspiration, Journal of Geophysical Research: Biogeosciences, 116, https://doi.org/10.1029/2010JG001463, https://agupubs.onlinelibrary.wiley.com/doi/abs/10.1029/2010JG001463, 2011.

Potchter, O., Cohen, P., and Bitan, A.: Climatic behavior of various urban parks during hot and humid summer in the mediterranean city of Tel Aviv, Israel, International Journal of Climatology, 26, 1695–1711, https://doi.org/10.1002/joc.1330, 2006.

Qiu, G.-Y., Li, H.-Y., Zhang, Q.-T., Chen, W., Liang, X.-J., and Li, X.-Z.: Effects of Evapotranspiration on Mitigation of Urban Temperature by Vegetation and Urban Agriculture, Journal of Integrative Agriculture, 12, 1307 – 1315, https://doi.org/https://doi.org/10.1016/S2095-3119(13)60543-2, http://www.sciencedirect.com/science/article/pii/S2095311913605432, 2013.

Redon, E., Lemonsu, A., Masson, V., Morille, B., and Musy, M.: Implementation of street trees within the solar radiative exchange parameterization of TEB in SURFEX v8.0, Geoscientific Model Development, 10, 385–411, https://doi.org/10.5194/gmd-10-385-2017, 2017.

Ryu, Y., Bou-Zeid, E., Wang, Z., and Smith, J.: Realistic Representation of Trees in an Urban Canopy Model, Boundary-Layer Meteorology, 159, 193–220, https://doi.org/10.1007/s10546-015-0120-y, 2016.

Salim, M., Schlünzen, K., and Grawe, D.: Including trees in the numerical simulations of the wind flow in urban areas: Should we care?, Journal of Wind Engineering and Industrial Aerodynamics, 144, 84 – 95, https://doi.org/https://doi.org/10.1016/j.jweia.2015.05.004, http://www.sciencedirect.com/science/article/pii/S0167610515001178, selected papers from the 6th International Symposium on Computational Wind Engineering CWE 2014, 2015.

Santiago, J. and Martilli, A.: A Dynamic Urban Canopy Parameterization for Mesoscale Models Based on Computational Fluid Dynamics Reynolds-Averaged Navier–Stokes Microscale Simulations, Boundary-Layer Meteorology, 137, 417–439, https://doi.org/10.1007/s10546-010-9538-4, 2010.

Shashua-Bar, L. and Hoffman, M.: Vegetation as a climatic component in the design of an urban street: An empirical model for predicting the cooling effect of urban green areas with trees, Energy and Buildings, 31, 221–235, https://doi.org/10.1016/S0378-7788(99)00018-3, 2000.

Shashua-Bar, L., Pearlmutter, D., and Erell, E.: The cooling efficiency of urban landscape strategies in a hot dry climate, Landscape and Urban Planning, 92, 179–186, https://doi.org/10.1016/j.landurbplan.2009.04.005, 2009.

Shashua-Bar, L., Pearlmutter, D., and Erell, E.: The influence of trees and grass on outdoor thermal comfort in a hot-arid environment, International Journal of Climatology, 31, 1498–1506, https://doi.org/10.1002/joc.2177, 2011.

Souch, C.: The effect of trees on summertime below canopy urban climates: a case study, Bloomington, Indiana, J. Arboric., 19, 1993.

Yamada, T.: A Numerical Model Study of Turbulent Airflow in and Above a Forest Canopy, Journal of the Meteorological Society of Japan. Ser. II, 60, 439–454, https://doi.org/10.2151/jmsj1965.60.1_439, 1982.
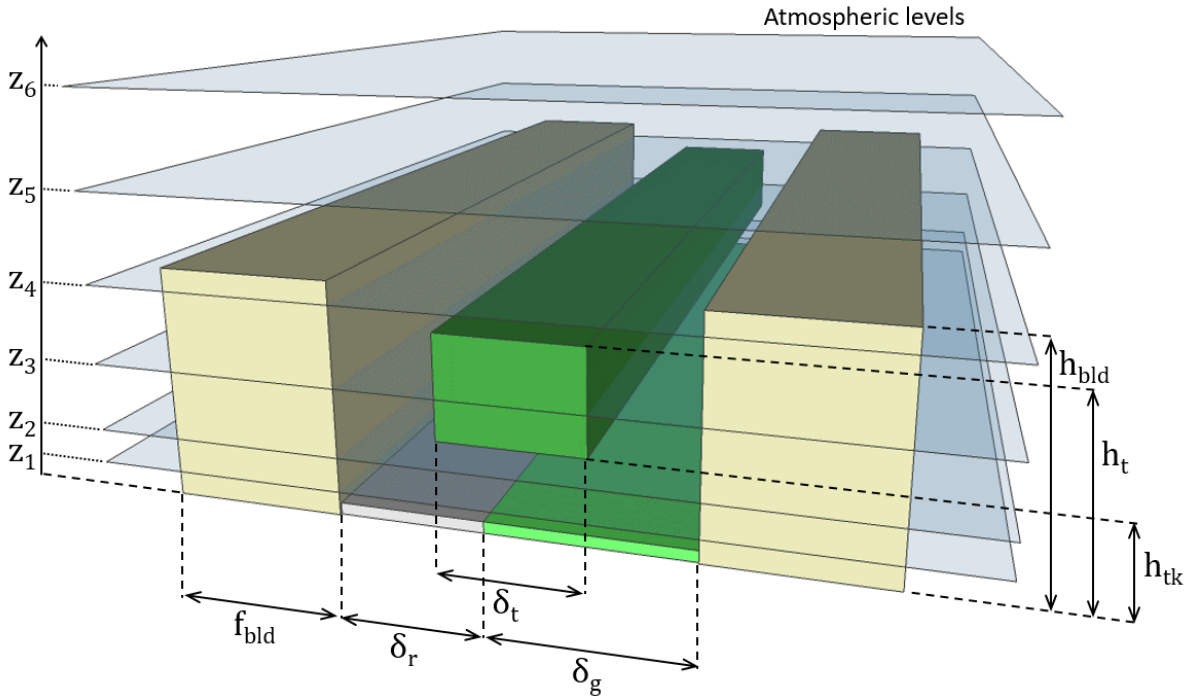
Figure 1. Schematic representation of the TEB's urban canyon integrating a part of ground-based natural covers and an explicit tree-foliage layer, and of the atmospheric vertical levels of the SBL scheme coupled to TEB to compute vertical profiles of micrometeorological variables inside and above the canyon.
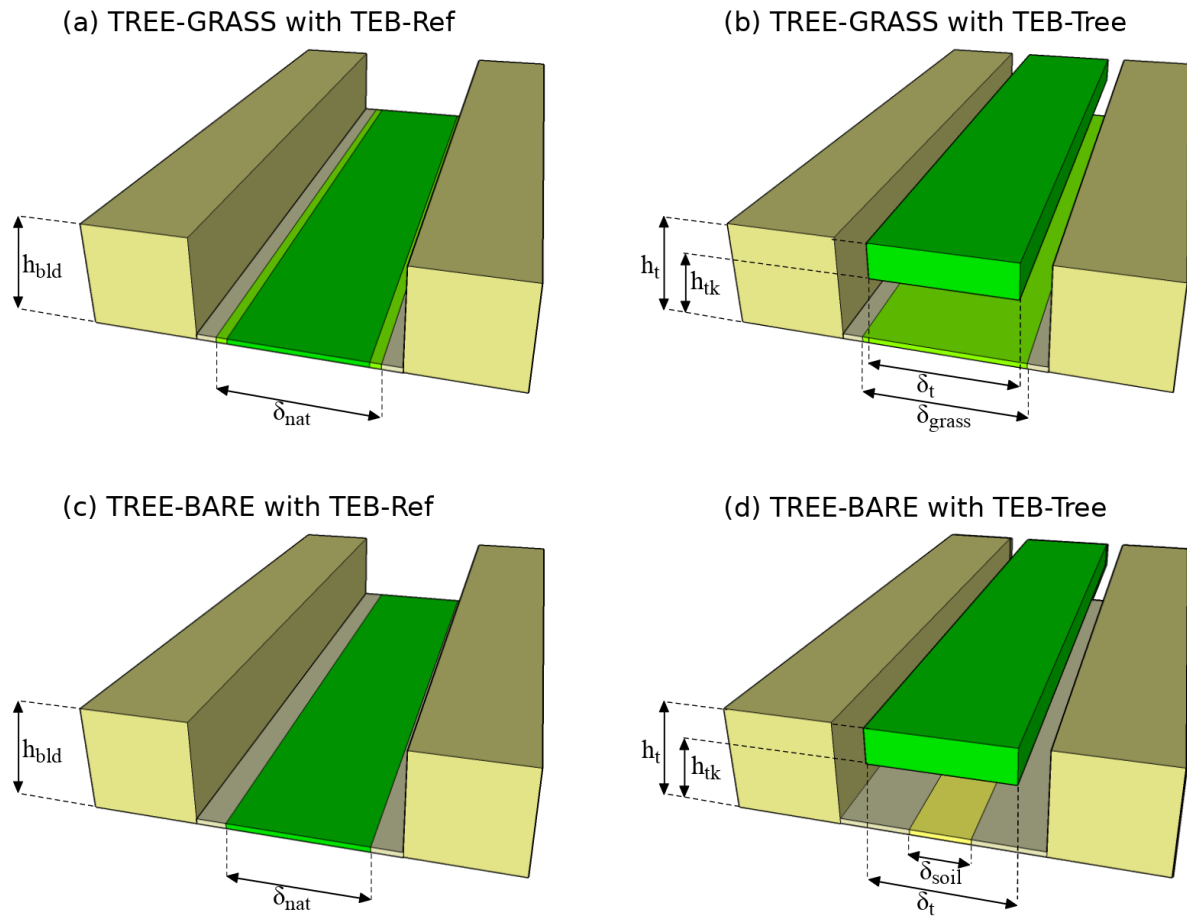
Figure 2. Comparison of urban canyon characteristics prescribed by TEB-Ref (left) and TEB-Tree (right) versions for the experiments TREE-GRASS (top) and TREE-BARE (bottom).
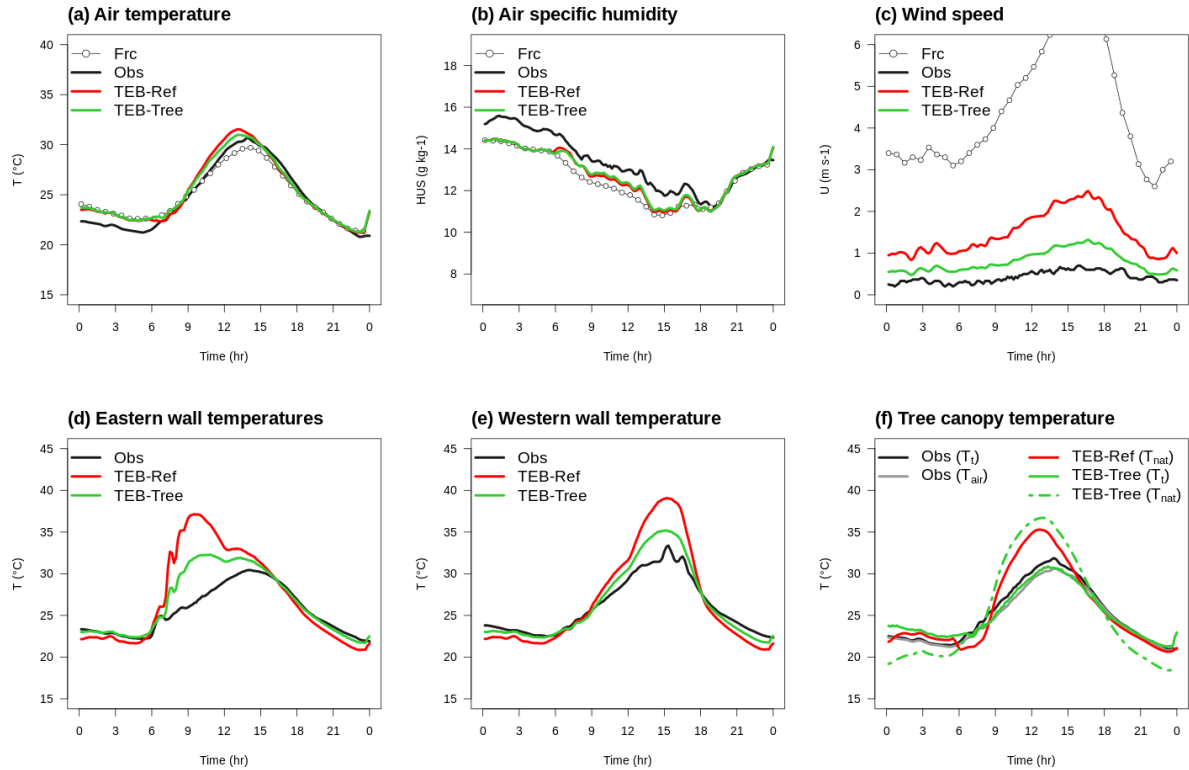
Figure 3. Comparison of the TEB-Ref and TEB-Tree results (red and green lines, respectively) with meteorological variables (top panel) and surface temperatures of urban facets and trees (bottom panel) measured within the courtyard (black line). For air temperature, specific humidity and wind speed, the gray line with symbols indicates the forcing data above the buildings.
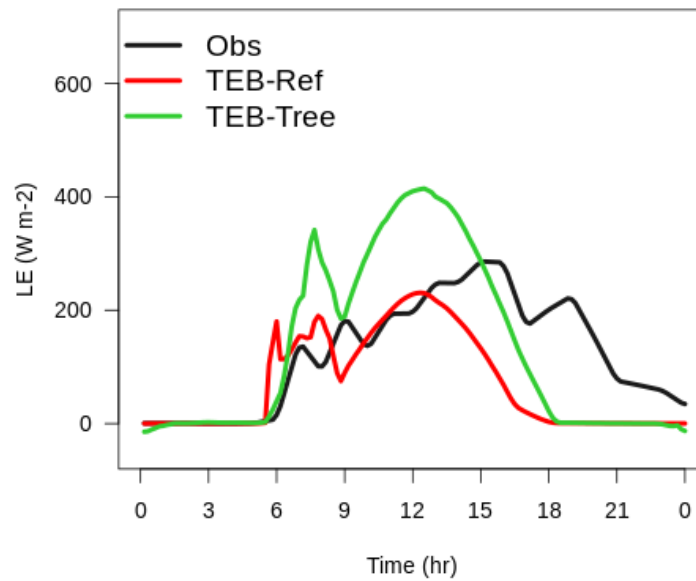
Figure 4. Comparison of the TEB-Ref and TEB-Tree results (red and green lines, respectively) with the latent heat flux deduced from measurements of tree transpiration and grass evaporation (black line).
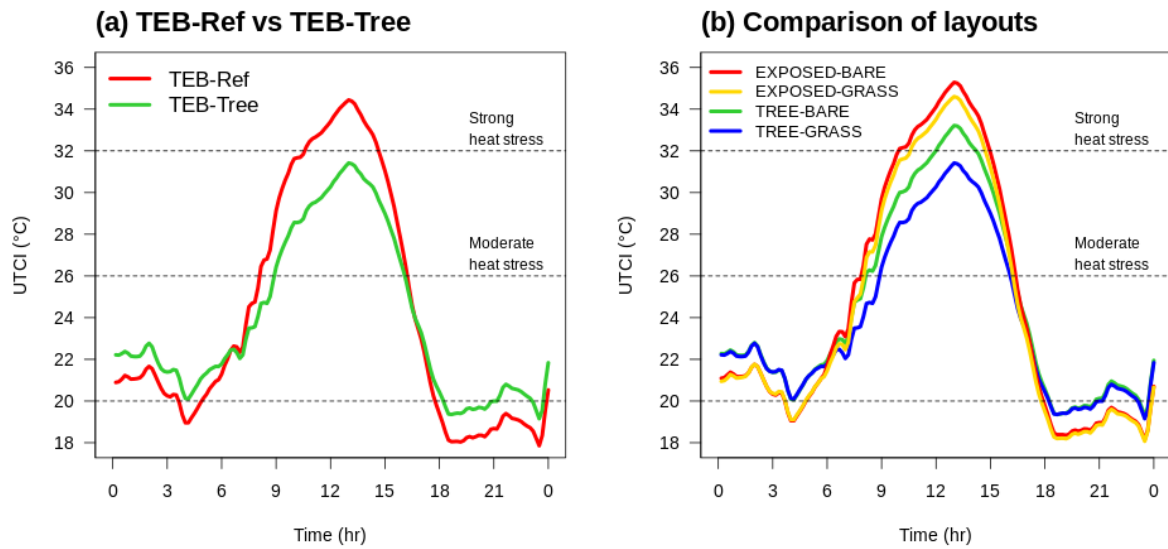
Figure 5. (a) Comparison of UTCI simulated in the courtyard by TEB-Ref (red line) and TEB-Tree (green line) for TREE-GRASS configuration; and (b) Comparison of UTCIs simulated by TEB-Tree for four different courtyard layouts.

Table 1. TEB's input parameters according to the two configurations prescribed to represent the experimental site of Sde-Boqer according to the TEB-Ref and TEB-Tree versions (in accordance with Figure 2).

		TREE-BARE		TREE-GRASS	
		TEB-Ref	*TEB-Tree*	*TEB-Ref*	*TEB-Tree*
Building fraction	(-)	0.350	0.350	0.350	0.350
Pavement fraction	(-)	0.195	0.450	0.130	0.130
Ground-based nature fraction	(-)	0.455	0.200	0.520	0.520
- High vegetation	(-)	1.000	-	0.875	-
- Low vegetation fraction	(-)	0.000	0.000	0.125	1.000
- Bare soil fraction	(-)	0.000	1.000	0.000	0.000
Tree overlapping fraction / canyon	(-)	-	0.700	-	0.700
Building height	(m)	3.0	3.0	3.0	3.0
Aerodynamic roughness length	(m)	0.3	0.3	0.3	0.3
Wall-plan area ratio	(-)	0.71	0.71	0.71	0.71
Canyon aspect ratio	(-)	0.55	0.55	0.55	0.55

Table 2. Mean absolute error (Model-Obs) and root-mean square error in temperature, humidity, and wind speed at 1.5 m agl, in surface temperature of walls and tree foliage, and in evaporation. The scores are calculated for TEB-Ref and TEB-Tree, and for the two courtyard configurations TREE-GRASS and TREE-BARE.

			TEB-Ref		*TEB-Tree*	
			MAE	RMSE	MAE	RMSE
TREE-GRASS	$T_{1.5m}$	(°C)	0.74	0.90	0.67	0.83
	$q_{1.5m}$	(g kg^{-1})	0.64	0.74	0.61	0.71
	$U_{1.5m}$	(m s^{-1})	1.05	1.12	0.37	0.41
	$T_{Swall_{(East)}}$	(°C)	2.52	4.02	1.21	2.04
	$T_{Swall_{(West)}}$	(°C)	2.03	2.82	0.90	1.28
	T_{Tree}	(°C)	1.32	1.84	0.71	0.85
	LE_{Tree}	(°C)	71.60	102.88	83.38	108.10
TREE-BARE	$T_{1.5m}$	(°C)	0.77	0.99	0.75	0.94
	$q_{1.5m}$	(g kg^{-1})	0.64	0.86	0.65	0.86
	$U_{1.5m}$	(m s^{-1})	1.02	1.14	0.57	0.64
	$T_{Swall_{(East)}}$	(°C)	3.01	4.21	1.30	2.08
	$T_{Swall_{(West)}}$	(°C)	2.68	3.23	1.02	1.46
	$T_{Spavement}$	(°C)	5.25	7.34	2.54	3.88
	T_{Tree}	(°C)	1.61	2.26	1.14	1.57
	LE_{Tree}	(°C)	12.76	15.49	16.92	21.60